

XMM-EPIC observation of MCG–6-30-15: direct evidence for the extraction of energy from a spinning black hole?

Jörn Wilms,^{1*} Christopher S. Reynolds,^{2,3,†} Mitchell C. Begelman,^{3,4} James Reeves,⁵ Silvano Molendi,⁶ Rüdiger Staubert¹ and Eckhard Kendziorra¹

¹*Institut für Astronomie und Astrophysik, Abt. Astronomie, Universität Tübingen, Sand 1, D-72076 Tübingen, Germany*

²*Department of Astronomy, University of Maryland, College Park, MD 20742, USA*

³*JILA, Campus Box 440, University of Colorado, Boulder, CO 80309, USA*

⁴*Department of Astrophysical and Planetary Sciences, University of Colorado, Boulder, CO 80309, USA*

⁵*X-Ray Astronomy Group, Department of Physics and Astronomy, Leicester University, Leicester LE1 7RH*

⁶*Istituto di Fisica Cosmica, CNR, via Bassini 15, I-20133 Milano, Italy*

Accepted 2001 October 22. Received 2001 October 22; in original form 2001 August 24

ABSTRACT

We present *XMM-Newton* European Photon Imaging Camera (EPIC) observations of the bright Seyfert 1 galaxy MCG–6-30-15, focusing on the broad Fe K α line at ~ 6 keV and the associated reflection continuum, which is believed to originate from the inner accretion disc. We find these reflection features to be *extremely* broad and redshifted, indicating an origin in the very central regions of the accretion disc. It seems likely that we have caught this source in the ‘deep minimum’ state first observed by Iwasawa et al. The implied central concentration of X-ray illumination is difficult to understand in any pure accretion disc model. We suggest that we are witnessing the extraction and dissipation of rotational energy from a spinning black hole by magnetic fields connecting the black hole or plunging region to the disc.

Key words: accretion, accretion discs – black hole physics – galaxies: individual: MCG–6-30-15 – galaxies: Seyfert – X-rays: galaxies.

1 INTRODUCTION

X-ray spectra of Seyfert 1 galaxies commonly show an iron K α emission line at ~ 6 keV. The line is often extremely broad, with a velocity width of $> 70\,000$ km s $^{-1}$. Furthermore, the asymmetries in the line profiles are well explained by relativistic effects. Both of these facts suggest that the line is emitted from the surface layers of the accretion disc within a few gravitational radii $r_g = GM/c^2$ of the black hole (BH) itself. It is now widely believed that this spectral feature is a relatively clean probe of the immediate environments of supermassive BHs (see Fabian et al. 2000, and references therein).

One of the best-studied broad iron line sources is the nearby bright Seyfert 1 galaxy MCG–6-30-15 ($z = 0.008$). This was the first active galactic nucleus (AGN) for which a relativistic iron line disc profile was measured. In their *Advanced Satellite for Cosmology and Astrophysics* (ASCA) observations, Tanaka et al. (1995) found that the iron line profile could be explained by emission from an accretion disc around a non-rotating (Schwarzschild) BH. In a detailed reanalysis, however, Iwasawa et al. (1996) found a much broader line during a period of low continuum X-ray flux, the so-called ‘deep minimum state’. The line becomes so

broad that disc models require emission from within $6r_g$, suggesting either a rotating (Kerr) BH, with its marginally stable orbit at $r_{ms} < 6r_g$ (Iwasawa et al. 1996; Dabrowski et al. 1997), or iron fluorescence from material spiralling into the BH at $< r_{ms}$ (Reynolds & Begelman 1997). Such a broad line was later confirmed, e.g. by Guainazzi et al. (1999) and Lee et al. (1999).

Using the new generation of X-ray satellites such as *XMM-Newton* with their improved collecting area and X-ray CCD spectral resolution, the Fe line of Seyferts can be studied in greater detail than was possible before. In this Letter, we present data from a 100 ks *XMM-Newton* observation of MCG–6-30-15.

2 INSTRUMENTATION AND DATA REDUCTION

Our observation covered most of orbit 108 of *XMM-Newton*, on 2000 June 11/12, and was simultaneous with the *Rossi X-ray Timing Explorer* (*RXTE*). Here, we report on data from the European Photon Imaging Cameras (EPIC) on board *XMM-Newton* (Strüder et al. 2001; Turner et al. 2001). To prevent photon pile-up, the EPIC-pn camera was operated in its small-window mode (using the medium thick filter to prevent optical light contamination), and the EPIC MOS-1 camera was operated in its timing mode. The MOS-2 camera was operated in full-frame

*E-mail: wilms@astro.uni-tuebingen.de

† Hubble Fellow while at the University of Colorado.

mode to study the field surrounding MCG–6-30-15. Although we primarily rely on the pn data here, the pile-up in the MOS-2 data can be reduced to < 5 per cent when using single events only. Therefore we can use the MOS-2 data to check for the instrument-independence of our results.

As of 2001 August, the official version of the *XMM-Newton* Science Analysis Software (SAS) contained only a preliminary model for the charge transfer efficiency (CTE) of the pn-chips. Therefore, we used an internal SAS version implementing an improved model for the EPIC-pn CTE (Haberl, private communication). To avoid remaining response matrix uncertainties, we concentrate on the energy range from 0.5 to 11 keV. To produce EPIC-pn source and background spectra, we collected events from two circles of radius 10 pixels on and off the source for those times when the source count rate was below 14 counts s^{-1} . This upper limit of the count rate is necessary to avoid phases where the core of the MCG–6-30-15 point spread function was slightly piled up. The total resulting EPIC integration time was 54 ks. We checked the background light curve for periods of severely increased background, but none was found.

For spectral modelling, response matrices appropriate for the improved CTE model and appropriate for the source position on the EPIC chip were used. Furthermore, we corrected the exposure time in the spectra for the ~ 71 per cent live time of the pn small-window mode (Kuster et al. 1999) and performed simultaneous fits with single and double events. We estimate that the overall uncertainties in the spectral calibration and flux calibration owing to these procedures are at most a few per cent.

3 THE IRON LINE PROFILE AND ACCRETION DISC FITS

Fig. 1(a) shows the ratio of the 0.5–11 keV EPIC-pn data to a spectral model consisting of a pure power law (fitted in the 2–11 keV band) modified by Galactic absorption ($N_{\text{H}} = 4.1 \times 10^{20} \text{ cm}^{-2}$, using the XSPEC PHABS model with cross-sections similar to those described by Wilms, Allen & McCray 2000). Below ~ 2 keV, there is significant spectral complexity which is due to a warm absorber (Nandra & Pounds 1994; Reynolds & Fabian 1995; Lee et al. 2001), possibly superposed with a complex of relativistically broadened soft X-ray recombination lines (Branduardi-Raymont et al. 2001). At 3–7 keV, a broad hump in the spectrum suggests the identification with disc reflection signatures and, especially, the broad iron $K\alpha$ line.

The putative broad iron line is more apparent once the soft X-ray spectral complexity has been modelled. This is not a trivial exercise since the physical nature of this complexity is still a matter of debate. To start with, we consider a warm absorber scenario (this will be generalized to include soft X-ray relativistic emission lines below). We assume that the continuum consists of a power law modified by Galactic absorption. We also allow for the possibility of intrinsic neutral absorption in MCG–6-30-15 (although the best-fitting column density is always consistent with zero). By fitting the high-resolution X-ray spectrum from the Reflection Grating Spectrograph (RGS), we construct an empirical warm absorber model (based on Lee et al. 2001) with absorption edges of C V, O VII, O VIII and Ne X (at 392, 740, 870 and 1362 eV, respectively, with best-fitting optical depths at threshold of $\tau = 0.34, 0.87, 1.17$ and 0.10), a Gaussian absorption feature below the O VII and O VIII edges to crudely model blended resonance absorption lines, and four moderately broad and weak Gaussian emission features at observed energies of 0.885, 0.935,

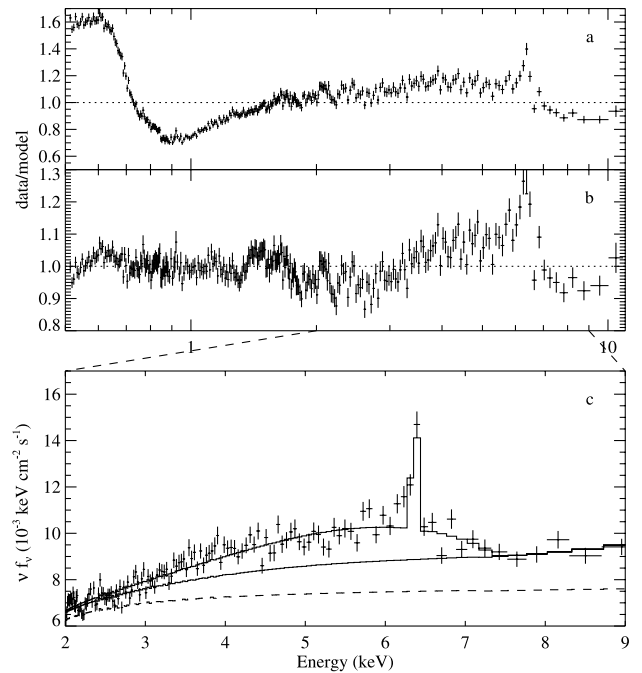


Figure 1. (a) Ratio between data and model from fitting a power law to the 0.5–11 keV data. (b) Ratio from fitting a power law and the empirical warm absorber model (see text). (c) Deconvolved spectrum of the Fe $K\alpha$ band, showing the total LAOR model and the continuum with and without (dashed) the reflection component for a model with reflection from an ionized disc. For clarity, the data have been rebinned and only the single-event data points are shown.

0.995 and 1.06 keV, which are merely included to fit the RGS data; we do not attempt to make a physical identification of these features. After applying this empirical model to the data, the soft X-ray residuals are reduced to less than 10 per cent, and the broad iron line feature is much more obvious (Fig. 1b). The best-fitting photon index is $\Gamma = 1.87 \pm 0.01$ (goodness of fit $\chi^2/\text{dof} = 2625/1719$, all uncertainties are quoted at the 90 per cent level for one interesting parameter, $\Delta\chi^2 = 2.71$).

We now consider the nature of the hard spectral complexity. While it may be tempting to model the hump-like feature as pure broad iron line emission, this is not a physically consistent model. The equivalent width of this feature (measured relative to the continuum at the iron $K\alpha$ rest-frame energy) is ~ 1 keV, and it would be impossible to obtain such a broad iron line without also observing the X-ray continuum photons that have been back-scattered from the accretion disc. Consequently, we will not present pure broad iron line models and jump, instead, to more physically motivated spectral models which include both iron line fluorescence and the backscattered ‘reflection’ continuum. Within the framework of such models, the 3–7 keV hump is a combination of iron line fluorescence and backscattered continuum photons (with the Fe K edge responsible for some fraction of the drop in flux at ~ 7 keV).

We construct a spectral model appropriate for the case of reflection from the Keplerian regions of an accretion disc around a near-extremal Kerr BH ($a = 0.998$). The inner edge of the X-ray reprocessing region is taken to be the radius of marginal stability, $r_{\text{ms}} = 1.23r_{\text{g}}$, and the outer edge is taken to be $r_{\text{out}} = 400r_{\text{g}}$. We fix the inclination of the inner disc to be $i = 30^\circ$ (Tanaka et al. 1995) and note that our results below only slightly depend on the value of

i chosen. We assume that the reflected emission has an emissivity profile $\epsilon \propto r^{-\beta}$ and leave β as a free parameter. The reflection continuum is described using the PEXRIV model of XSPEC and normalized to the case where the accretion disc intercepts half of the X-ray power-law continuum photons (i.e. $R = 1$). Both the iron line profile and the reflection continuum are then relativistically smeared [using the model of Laor (1991) as the kernel]. Here, and throughout the rest of the spectral modelling discussed in this paper, we also include a narrow (unresolved) Gaussian line at 6.4 keV with equivalent width $W_{K\alpha,N}$ to model the obvious narrow-line core. This component presumably originates from distant material such as the putative molecular torus of Seyfert unification schemes, and has recently been seen in several other AGN [e.g. in NGC 5548 (Yaqoob et al. 2001) or in Mrk 205 (Reeves et al. 2001)].

First, we consider the case of a fairly cold accretion disc (rest-frame iron line energy of 6.4 keV, disc ionization parameter $\xi = 1$, and $R = 1$). The resulting best-fitting parameters are $\Gamma = 2.09 \pm 0.01$, $\beta = 3.6 \pm 0.1$, $W_{K\alpha,N} = 38$ eV and $W_{K\alpha,B} = 805$ eV ($\chi^2/\text{dof} = 2383/1717$). However, this model fails to explain the data as well as possessing an unphysically large broad-line equivalent width. Significant residuals (up to ~ 20 per cent) remain in the 3–11 keV band. The pattern of residuals suggests that the model is failing to produce the red wing of the 3–7 keV hump, and is underestimating the flux in the blueward edge of this feature. A hard tail above 8 keV suggests that we are also underestimating the strength of the high-energy reflection continuum. If we allow the relative normalization of the reflection continuum, R , to be a free parameter, the fit converges to a very large value of R ($R = 7.6_{-1.3}^{+1.8}$, also $\Gamma = 2.35 \pm 0.05$ and $\beta = 4.4 \pm 0.2$, $\chi^2/\text{dof} = 2055/1716$). Despite the slightly better χ^2 , large residuals around ~ 7 keV remain.

Ionization of the accretion disc surface is another way of increasing the amount of reflection continuum. To model this (with the relative normalization of the reflection continuum fixed to $R = 1$), we allow the ionization parameter of the disc ξ , the temperature of the disc T and the energy of the iron line E to be free parameters (E is constrained to lie in the range of allowable Fe $K\alpha$ energies: 6.40 to 6.97 keV). The resulting best fit has $\Gamma = 2.00 \pm 0.02$, $\beta = 3.29_{-0.11}^{+0.12}$, $E = 6.40_{-0}^{+0.05}$ keV, $\xi = 1380_{-190}^{+570}$, $T > 6.0 \times 10^5$ K, $W_{K\alpha,N} = 41$ eV and $W_{K\alpha,B} = 235$ eV ($\chi^2/\text{dof} = 2051/1714$). This leads to a significantly better fit with the higher iron edge/line energies explaining the residual at ~ 7 keV. However, significant residuals still exist in the 3–5 keV range (suggesting that we are still under-predicting the flux in the red wing of the reflection feature) and above 8 keV.

Detailed examination of this last spectral model shows that features in the *soft* X-ray band below 1.5 keV determine the best-fitting ionization parameter and temperature. Consequently, such fits must be viewed with suspicion – there are a number of physical processes that are not included in this reflection model but which may well contribute to the soft X-ray spectrum (most notably, the recombination line and edge emission from C, N, O and Ne). It would also not be surprising if our empirical warm absorber model left small soft X-ray residuals which may then be mistakenly fitted by ionized reflection models.

First, we can consider the ionized reflection fits ignoring all data below 1.5 keV. Refitting the ionized disc model (including the empirical warm absorber) to the 1.5–11 keV band results in a good fit with no clear residuals. The best-fitting parameters are $\Gamma = 1.94 \pm 0.02$, $\beta = 4.6 \pm 0.3$, $E = 6.95_{-0.15}^{+0}$ keV, $W_{K\alpha,N} = 51$ eV and $W_{K\alpha,B} = 582$ eV ($\chi^2/\text{dof} = 1506/1312$). T and ξ are

unconstrained by the data, while the relative normalization of the reflection continuum is constrained to be $R < 4.7$. During the fitting R is anti-correlated with $W_{K\alpha,B}$. These quantities are physically consistent with each other (i.e. the iron line has the appropriate strength for that value of R and ξ) when $R \sim 1.5$ –2 (corresponding to $W_{K\alpha,B} \sim 300$ –400 eV).

This spectral modelling suggests that the accretion disc may be ionized. Consequently, the $K\alpha$ line need not be intrinsically narrow as we have assumed so far, but might be Compton-broadened in the hot skin of the accretion disc [note that Compton broadening alone cannot explain the large line width (Reynolds & Wilms 2000)]. We examine this possibility by relaxing our assumption of a narrow intrinsic line and, instead, model the *intrinsic* iron line with a Gaussian profile of width σ . Using the 1.5–11 keV data, the best-fitting value is $\sigma = 0$ (with other parameters as above). Even if we force the line to be very broad (e.g. $\sigma = 1$ keV, at the expense of reducing the goodness of fit by $\Delta\chi^2 = 13$), the data still require $\beta > 3.9$.

The second approach for handling the soft X-ray spectrum is to model explicitly the recombination K lines of C, N, O and Ne. Qualitatively, this model is the same as the mixed emission-line model of Branduardi-Raymont et al. (2001) with the presence of additional warm absorption. The best-fitting parameters are $\Gamma = 1.96 \pm 0.01$, $\beta = 4.70_{-0.27}^{+0.25}$, $E = 6.97_{-0.10}^{+0}$ keV, $W_{K\alpha,N} = 53$ eV, $\xi > 130$ and $W_{K\alpha,B} = 546$ eV ($\chi^2/\text{dof} = 1907/1704$). Again, the relative reflection normalization is poorly constrained by these data, but self-consistency is achieved for $R \sim 1.5$ –2 and $W_{K\alpha,B} \sim 300$ –400 eV. We conclude that the parametrization of the soft energy spectrum does not qualitatively change the results for the broadened Fe $K\alpha$ line.

We note that the PEXRIV reflection model employed here is also incomplete because of the neglect of Compton smearing of the absorption edges. We do not expect this to seriously compromise our results since the observed smearing is much greater than that expected from Compton effects. However, we will examine these effects using improved models (Ballantyne, Iwasawa & Fabian 2001; Nayakshin & Kallman 2001) in a future publication. Preliminary investigations show our current conclusions to be robust. Finally, to check the dependence of these results on possible remaining calibration uncertainties, we used the data from the MOS-2 camera. The best-fitting parameters that we find are consistent to within the error bars, with slight deviations at the Si edge which are a known calibration issue. We conclude that our results are independent of any remaining calibration issues with the EPIC instruments.

To summarize, our physically motivated best-fitting model consists of reflection from an ionized accretion disc that emits H-like iron $K\alpha$ fluorescence with a relative reflection fraction of $R \approx 1.5$ –2 and a broad iron line equivalent width of $W_{K\alpha,B} \approx 300$ –400 eV. The 2–10 keV flux of $F_{2-10} = 2.3 \times 10^{-11}$ erg s $^{-1}$ cm $^{-2}$ is comparable with the ‘deep minimum state’ found by Iwasawa et al. (1996, $F_{2-10} = 2.0 \times 10^{-11}$ erg s $^{-1}$ cm $^{-2}$). *The most interesting feature of these spectral models is that a very steep emissivity profile $\beta = 4.3$ –5.0 for the iron-line/reflection features is required.* We address the implications of this result in the next section.

Finally, we note that if r_{in} is allowed to vary, the data require $r_{in} < 2.1r_g$ in order to model the red wing of the 3–8 keV hump. We explicitly note that the data cannot be adequately described by any reflection model with an inner radius of $r_{in} = 6r_g$, the radius of marginal stability around a Schwarzschild BH. Thus models in which the X-ray reflection occurs in the Keplerian part of accretion

discs around a non-rotating BH cannot explain these data. In principle, there can be X-ray reflection inside the radius of marginal stability (Reynolds & Begelman 1997). However, as discussed below, the extremely steep emissivity index β required by our data is very hard to understand in the context of Schwarzschild geometry.

4 DISCUSSION

Very steep emission profiles are required in all of our good fits to the Fe $K\alpha$ line and reflection continuum. Here, we explore the implications of this result, assuming that the reflected flux (including the iron line) from a local patch of the disc is proportional to the X-ray continuum flux (at the iron K-shell edge) irradiating that patch. We will assume that a fixed fraction f of the energy released locally in the body of the accretion disc is transported into an accretion disc corona and then radiated in the X-ray band. Studies of such coronae suggest that $f \sim 1$ in order to produce the observed continua (Haardt & Maraschi 1993; Dove et al. 1997). Thus, while our assumption may not be true in detail, it must be approximately true across a wide range of disc radii.

4.1 Accretion disc models

Can standard BH accretion disc models (Novikov & Thorne 1973; Riffert & Herold 1995) explain the observed emissivity profiles? With the assumptions described above, this question reduces to an examination of the radial distribution of energy dissipation in such disc models. For a disc around an $a = 0.998$ BH, the flux emitted from the disc per unit proper area of the disc, $\mathcal{E}(r)$, peaks at $r \sim 1.6r_g$ and then gradually steepens to approach $\mathcal{E}(r) \propto r^{-3}$. At no point does $\mathcal{E}(r)$ become as steep as $r^{-4.5}$, as required by our iron line observations. This is true for any assumed BH spin. Also, as noted above, the emissivity profile is steeper than accretion disc models even if one accounts for intrinsic broadening of the iron line via Comptonization.

We note that there are two complications that may be relevant to real discs, even though they go beyond the realm of standard disc models. First, magnetic fields might couple material within $r = r_{\text{ms}}$ to the rest of the disc, thereby permitting continued energy extraction from this material (Gammie 1999; Krolik 1999; Agol & Krolik 2000, hereafter AK00). Non-relativistic accretion disc simulations employing pseudo-Newtonian potentials suggest that the stresses and presumably the dissipation remain fairly flat within this region (Hawley & Krolik 2001; Armitage, Reynolds & Chiang 2001). Hence it would seem that the required emissivities are difficult to achieve through such effects for discs around Schwarzschild holes. Secondly, X-rays produced away from the equatorial plane might be gravitationally focused into the central regions of the disc. However, using the method of Petrucci & Henri (1997), we find that such effects cannot produce the observed emissivity profile unless the X-ray source is already situated in the very central regions of the disc.

We conclude that the disc has to be irradiated in a more centrally concentrated manner than predicted by current pure accretion disc models. In other words, we require some additional X-ray source that is both powerful and very centrally concentrated. There is one obvious candidate: *X-rays that are associated with the magnetic extraction of BH spin energy.*

4.2 Magnetic extraction of BH spin energy

Here, we explore the suggestion that the central X-ray source is associated with the extraction of BH spin energy, focusing on scenarios in which the BH spin is extracted via magnetic fields that pierce the (stretched) event horizon (Blandford & Znajek 1977). An alternative class of models in which the magnetic fields do not pierce the horizon will be addressed below. In order to produce the required steep irradiation profile, the X-ray production must occur close to the disc itself with a production rate that is a steeply declining function of radius. Thus we are led to consider models in which the magnetic field lines connect the rotating event horizon to the accretion disc and/or disc corona. For definiteness, we will consider the canonical near-extremal Kerr BH.

In models in which the magnetic field lines are strongly coupled to the body of the accretion disc, the magnetic field transmits a retarding couple to the BH if the BH rotates faster than the magnetically connected region of the disc where the extracted rotational energy will be deposited. In order to power the observed X-ray source, the field strength close to the BH needs to be $B \sim 10^4 \text{ G} (M/10^7 M_\odot)^{-1}$ (Blandford & Znajek 1977). This is not an impossibly high field; the corresponding magnetic pressure is still substantially below the ram pressure of the accretion flow within r_{ms} and so can be confined to the BH region.

If a ring within the disc of width δr is connected to the event horizon with magnetic flux $\delta\Psi$, then the power dumped into the ring is (setting $GM_{\text{BH}} = c = 1$)

$$\delta P = \frac{(\delta\Psi)^2 \Omega_{\text{D}}(\Omega_{\text{H}} - \Omega_{\text{D}})}{4\pi^2 \delta r (-dZ_{\text{BH}}/dr)}, \quad (1)$$

where $\Omega_{\text{D}}(r) = (r^{3/2} + a)^{-1}$ is the angular velocity of the accretion disc, and the angular velocity of the event horizon is $\Omega_{\text{H}} = 0.479$ (Li 2000). The BH resistance, Z_{BH} , is a function of disc radius, r , defined by a map from the BH horizon to the accretion disc along the magnetic field lines. Viscous forces then transport this energy *outwards* by some distance before it is dissipated and radiated. AK00 and Li (2000) examine this process in detail and compute the radial dependence of the energy dissipation when the magnetic field connects to the accretion disc at one particular radius. We can use the formulae of AK00 (also see Li 2000) as the Green's function for computing the more general case.

It is beyond the scope of this Letter to address the detailed distribution of the hole-threading magnetic field across the disc surface, $B(r)$, or the nature of $Z_{\text{BH}}(r)$. If all of the extracted spin energy is dumped into a ring at $r = r_{\text{ms}}$, the emissivity is very steep ($\beta > 6$) within $r < 1.8r_g$ and gradually flattens to $\mathcal{E} \propto r^{-3.5}$ at large radius (Li 2000). More generally, the spin energy will be deposited into a range of radii, flattening this profile. We will assume $dZ_{\text{BH}}/dr \propto r^{-\nu}$ and $d\Psi/dr \propto r^{-\mu}$ ($\mu = 2$ corresponds to a dipole field for $r \gg 1$). For $\nu = 1$ and $\mu = 2$, $\mathcal{E} \propto r^{-3}$ at $r = 2r_g$ and is flatter inside that radius. To produce emission profiles as extreme as those required by our data (i.e. $\beta \sim 4.5$ at $r \sim 1.5r_g$), field configurations must be as concentrated as $\mu \sim 3-4$ (with some dependence on ν). Such conditions could be achieved, for example, if the field were 'pinned' on to the BH by the ram pressure of the accretion flow.

We note that the models addressed by AK00 do not employ the Blandford–Znajek effect but, instead, magnetically torque the disc via coupling to *matter* deep within the plunging region. For parameters relevant to our discussion, the extra energy source is provided by the BH spin via the Penrose effect occurring within the

radius of marginal stability (but outside the stretched horizon). In this case, all of the extra torque is provided at the inner edge of the disc (rather than across a range of radii as addressed above) and so a steep emissivity profile is a natural outcome.

Finally, we note that the large self-consistent value of $R \sim 1.5-2$ may have its origin in general relativity. Some fraction $f_{\text{ret}} < 0.5$ of the upwardly directed disc emission will be bent by the strong gravity and strike the disc again ('returning radiation': Cunningham 1975; Speith, Riffert & Ruder 1995; AK00), further enhancing $W_{\text{K}\alpha,\text{B}}$. This can enhance the relative amount of reflection by up to a factor of 2. Further computations are required to assess the effect of returning radiation on the emissivity profile in a self-consistent manner.

5 CONCLUSIONS

We have presented *XMM-Newton*-EPIC observations of MCG–6-30-15 containing a spectral feature that is best described as an extremely broad and redshifted X-ray reflection feature. On the basis of both the extreme spectrum and the source flux, it seems likely that we have caught MCG–6-30-15 in the peculiar 'deep minimum' state first noted by *ASCA* (Iwasawa et al. 1996). The extreme nature of the line profile leads us to conclude that it originates from the most central parts of the accretion disc. Standard accretion disc models cannot produce an emissivity profile that is centrally concentrated enough to produce the observed feature. It also seems unlikely that gravitational focusing of the continuum X-rays or magnetic coupling of the plunging region to the rest of the disc can ameliorate this conclusion. Therefore we suggest that, during the deep minimum state, X-rays associated with the magnetic extraction of the spin energy of the black hole are dominating the emission, producing a sufficiently compact source to explain our observations. Our results thus confirm the suggestion of Iwasawa et al. (1996) and Dabrowski et al. (1997) that MCG–6-30-15 possesses a rapidly rotating black hole.

In a forthcoming paper, we will present a more detailed analysis of our observation, including simultaneous fits with the *RXTE* Proportional Counter Array, a study of the time dependence of the reflection features and the X-ray continuum, and fits using a larger and more detailed set of continuum and reflection models.

ACKNOWLEDGMENTS

We thank A. C. Fabian, F. W. Haberl, J. H. Krolik and M. Kuster for useful conversations, and the referee, Chris Done, for her very prompt reply and useful comments. We acknowledge support from DLR grant 50 OX 0002 (JW, RS, EK), Hubble Fellowship grant HF-01113.01-98A (CSR) and NSF grant AST 98-76887 (CSR,

MCB). This work is based on observations obtained with *XMM-Newton*, an ESA science mission with instruments and contributions directly funded by ESA Member States and the USA (NASA).

REFERENCES

- Agol E., Krolik J. H., 2000, *ApJ*, 528, 161, (AK00)
 Armitage P. J., Reynolds C. S., Chiang J., 2001, *ApJ*, 548, 868
 Ballantyne D. R., Iwasawa K., Fabian A. C., 2001, *MNRAS*, 323, 506
 Blandford R. D., Znajek R. L., 1977, *MNRAS*, 179, 433
 Branduardi-Raymont G., Sako M., Kahn S. M., Brinkman A. C., Kaastra J. S., Page M. J., 2001, *A&A*, 365, L140
 Cunningham C. T., 1975, *ApJ*, 202, 788
 Dabrowski Y., Fabian A. C., Iwasawa K., Lasenby A. N., Reynolds C. S., 1997, *MNRAS*, 288, L11
 Dove J. B., Wilms J., Maisack M. G., Begelman M. C., 1997, *ApJ*, 487, 759
 Fabian A. C., Iwasawa K., Reynolds C. S., Young A. J., 2000, *PASP*, 112, 1145
 Gammie C. F., 1999, *ApJ*, 522, L57
 Guainazzi M. et al., 1999, *A&A*, 341, L27
 Haardt F., Maraschi L., 1993, *ApJ*, 413, 507
 Hawley J. F., Krolik J. H., 2001, *ApJ*, 548, 348
 Iwasawa K. et al., 1996, *MNRAS*, 282, 1038
 Krolik J. H., 1999, *ApJ*, 515, L73
 Kuster M., Benlloch S., Kendziorra E., Briel U. G., 1999, in Siegmund O. H., Flanagan K. A., eds, *EUV, X-ray and Gamma-Ray Instrumentation for Astronomy X*. SPIE, Bellingham, WA, p. 673
 Laor A., 1991, *ApJ*, 376, 90
 Lee J. C., Fabian A. C., Brandt W. N., Reynolds C. S., Iwasawa K., 1999, *MNRAS*, 310, 973
 Lee J. C., Ogle P. M., Canizares C. R., Marshall H. L., Schulz N. S., Morales R., Fabian A. C., Iwasawa K., 2001, *ApJ*, 554, L13
 Li L.-X., *ApJ*, 2000, submitted (astro-ph/0012469)
 Nandra K., Pounds K. A., 1994, *MNRAS*, 268, 405
 Nayakshin S., Kallman T. R., 2001, *ApJ*, 546, 406
 Novikov I. D., Thorne K. S., 1973, in DeWitt C., DeWitt B., eds, *Black Holes – Les Astres Occlus*. Gordon and Breach, New York, p. 345
 Petrucci P. O., Henri G., 1997, *A&A*, 326, 99
 Reeves J. N. et al., 2001, *A&A*, 365, L134
 Reynolds C. S., Begelman M. C., 1997, *ApJ*, 487, 109
 Reynolds C. S., Fabian A. C., 1995, *MNRAS*, 274, 1167
 Reynolds C. S., Wilms J., 2000, *ApJ*, 533, 812
 Riffert H., Herold H., 1995, *ApJ*, 450, 508
 Speith R., Riffert H., Ruder H., 1995, *Comput. Phys. Commun.*, 88, 109
 Strüder L. et al., 2001, *A&A*, 365, L18
 Tanaka Y. et al., 1995, *Nat*, 375, 659
 Turner M. J. L. et al., 2001, *A&A*, 365, L27
 Wilms J., Allen A., McCray R., 2000, *ApJ*, 542, 914
 Yaqoob T., George I. M., Nandra K., Turner T. J., Serlemitsos P. J., Mushotzky R. F., 2001, *ApJ*, 546, 759

This paper has been typeset from a $\text{\TeX}/\text{\LaTeX}$ file prepared by the author.